Hindawi
Mathematical Problems in Engineering
Volume 2021, Article ID 2942808, 11 pages
https://doi.org/10.1155/2021/2942808

Research Article

A Machine Learning-Based Big EEG Data Artifact Detection and Wavelet-Based Removal: An Empirical Approach

Shalini Stalin,[1] Vandana Roy,[2] Prashant Kumar Shukla,[3] Atef Zaguia,[4] Mohammad Monirujjaman Khan,[5] Piyush Kumar Shukla,[6] and Anurag Jain[7]

[1]*IIIT-Bhopal, M.P., Bhopal, India*
[2]*Department of Electronics and Communication, GGITS, Jabalpur 482002, M. P., India*
[3]*Department of Computer Science and Engineering, KL University, Vijayawada, Andhra Pradesh, India*
[4]*Department of Computer Science, College of Computers and Information Technology, Taif University, Taif 21944, Saudi Arabia*
[5]*Department of Electrical and Computer Engineering, North South University, Bashundhara, Dhaka 1229, Bangladesh*
[6]*Computer Science & Engineering Department, University Institute of Technology, Rajiv Gandhi Proudyogiki Vishwavidyalaya, (Technological University of Madhya Pradesh), Bhopal 462023, India*
[7]*Department of Computer Science and Engineering, Radharaman Engineering College, Bhopal, M.P., India*

Correspondence should be addressed to Mohammad Monirujjaman Khan; monirujjaman.khan@northsouth.edu

Received 9 July 2021; Revised 10 September 2021; Accepted 13 September 2021; Published 7 October 2021

Academic Editor: A. M. Bastos Pereira

The electroencephalogram (EEG) signals are a big data which are frequently corrupted by motion artifacts. As human neural diseases, diagnosis and analysis need a robust neurological signal. Consequently, the EEG artifacts' eradication is a vital step. In this research paper, the primary motion artifact is detected from a single-channel EEG signal using support vector machine (SVM) and preceded with further artifacts' suppression. The signal features' abstraction and further detection are done through ensemble empirical mode decomposition (EEMD) algorithm. Moreover, canonical correlation analysis (CCA) filtering approach is applied for motion artifact removal. Finally, leftover motion artifacts' unpredictability is removed by applying wavelet transform (WT) algorithm. Finally, results are optimized by using Harris hawks optimization (HHO) algorithm. The results of the assessment confirm that the algorithm recommended is superior to the algorithms currently in use.

1. Introduction

An effective diagnosis and analysis of neurological diseases are possible when a vital neurological signal is acquired from the patient. However, this signal is apprehended even in the highly hospitably environment and besmirched by some nonphysiological signals (artifacts). The most vital neurophysiological signal is electroencephalography (EEG) which represents the human brain electrical activities. Therefore, mitigation of these artifacts from EEG signals is a vibrant topic for research [1].

Different algorithms are applied for this EEG artifacts' suppression [2]. These motion artifacts are superimposed on the EEG signal. Thus, algorithms based on source separation must be applied for effective artifacts' elimination [3]. The EEG signal decomposition is done through the EEMD algorithm [4–9]. The blind source separation (BSS) approach is extensively used for artifacts' mitigation [10–15]. Additional, the most broadly applied algorithm is the wavelet transform [16–18] for EEG artifact elimination. The algorithms applied to detect artifacts from EEG signals are discussed in [19, 20] to better classify artifacts from EEG signals.

Experimentation is done on synthesized data which is detailed in [21]. The Ground-Truth (GT) EEG data is considered from online open resources [22].

1.1. Synthesized Artifact Signal Generation. A more accurate artifact removal method is developed in this research work and applied to remove motion artifacts, as this artifact is the most recurrent and distressing component in the EEG data.

However, this GT signal only is not capable to relate the effectiveness of the artifact elimination procedure. The simulated data consist of GT EEG data and an artifact template (which can be manually produced or separately chronicled). The simulated or synthesized data are created by adding this artifact template to the GT signal. Thus, the simulated data will be more effective because, after artifact removal, the signal can be compared with pure signal and the artifact elimination algorithm effectiveness is checked. These motion artifacts are generated synthetically by simulation. They are created by adding random noise sequences to the amplitude modulated EEG signal to be clearly seen in the EEG signal as artifacts.

These motion artifacts thoroughly distress the EEG data quality. Therefore, effective suppression is highly recommended before any neurological disorder diagnosis and analysis. Various artifact removal algorithms are applied to suppress these artifacts in the state-of-the-art research. However, the most suitable and efficient algorithms are applied in this recommended work to mitigate these artifacts effectively.

In this recommended work, ensemble empirical mode decomposition (EEMD) [9], blind source separation (BSS) [13], and wavelet transform (WT) [16] are applied in cascade for effective elimination of these motion artifacts. For removing the randomness and unpredictability of motion artifacts, the wavelet transform is more effective [7]. Finally, results are optimized by using Harris hawks optimization (HHO) algorithm.

A detailed architecture of the recommended methodology based on these algorithms is discussed in Section 2.

2. Recommended System Model

As shown in Figure 1, a system model is used to show a schematic representation of the recommended algorithm.

In this recommended work, primarily, the synthesized artifactual signal is preprocessed to eliminate the line and external noises [23]. Furthermore, these signals are decomposed through the EEMD approach. The decomposition is done for both pure EEG data and artifact-contaminated EEG data to generate IMFs. These generated IMFs are passes to the support vector machine (SVM) classifier for training. Subsequently, this classifier is used for the detection of motion artifacts from EEG. Once artifacts are identified, subsequently, the IMFs generated are sourced to a cascaded approach of CCA and SWT algorithm for purifying [24]. This cascaded algorithm will take some more time to execute. However, in medical diagnosis, this increased time is considerable. This approach is applied in an automated system where artifacts are automatically identified and removed with the most efficient algorithm to attain a clean signal [25].

2.1. Recommended Algorithm. The main goal of the recommended procedure is to remove the motion artifacts. Moreover, the neural information must be preserved after this EEG artifact removal. The recommended algorithm is divided into five categories. The details of the stages are given below [26]:

(i) Preprocessing: first, EEG data available as an online open-source interface [22] are preprocessed through a third-order butter worth filter for baseline wandering with two passband frequencies of 0.5 Hz to 99 Hz.

(ii) Synthetic artifact generation: the preprocessed signal of 120 datasets is considered as the ground-truth signal. Each data set contains 10000 samples. Furthermore, synthesized data are prepared by creating artifact templates of sinusoids and simulating these templates with a different amplitude, duration, and location and, finally, superimposed these templates onto the ground-truth signal. This artifact-contaminated EEG signal set also has 120 datasets with 10000 samples in each dataset [27].

(iii) Motion artifact detection: the motion artifact detection from single-channel artifact-contaminated EEG data has been carried out in two stages.

2.1.1. Decomposition Using EEMD. The preprocessed EEG signal is decomposed by using EEMD algorithm [9, 28].

2.1.2. Motion Artifact Detection Using SVM. These generated IMFs are used to attain statistical features such as kurtosis, mean, skewness, and variance, as discussed in [29]. These features are applied to support vector machine (SVM) to detect motion artifacts from EEG data.

2.1.3. Motion Artifact Removal. Once the artifact is detected in EEG data, artifacts' EEG data IMFs are applied to a cascaded approach of CCA-SWT for effective mitigation of EEG motion artifact. These correlation components (CCs) generated by the CCA algorithm are created based on self-correlation and uncorrelation. Statistically, uncorrelated components have distinguished properties. Threshold outputs are reconstructed through inverse wavelet transform to obtain external noise-free CCs. *Reconstruction*. Subsequently, the CCs having motion artifacts source are identified by using Pearson's correlation coefficients as the threshold. The CCs having less than the threshold value are rejected. Artifact-free EEG signal is obtained by reconstructing the remaining CCs from the original EEG signal.

2.1.4. Optimization. The irregularity which is introduced due to artifacts in EEG signal is removed by using the efficient methodology and finally optimized by Harris hawks optimization (HHO) algorithm.

3. Experiments

In this experiment, synthesized EEG signal is generated and processed with recommended cascaded algorithm to eradicate the diminishing effect of the motion artifact on the EEG data. Furthermore, the recommended algorithm results have

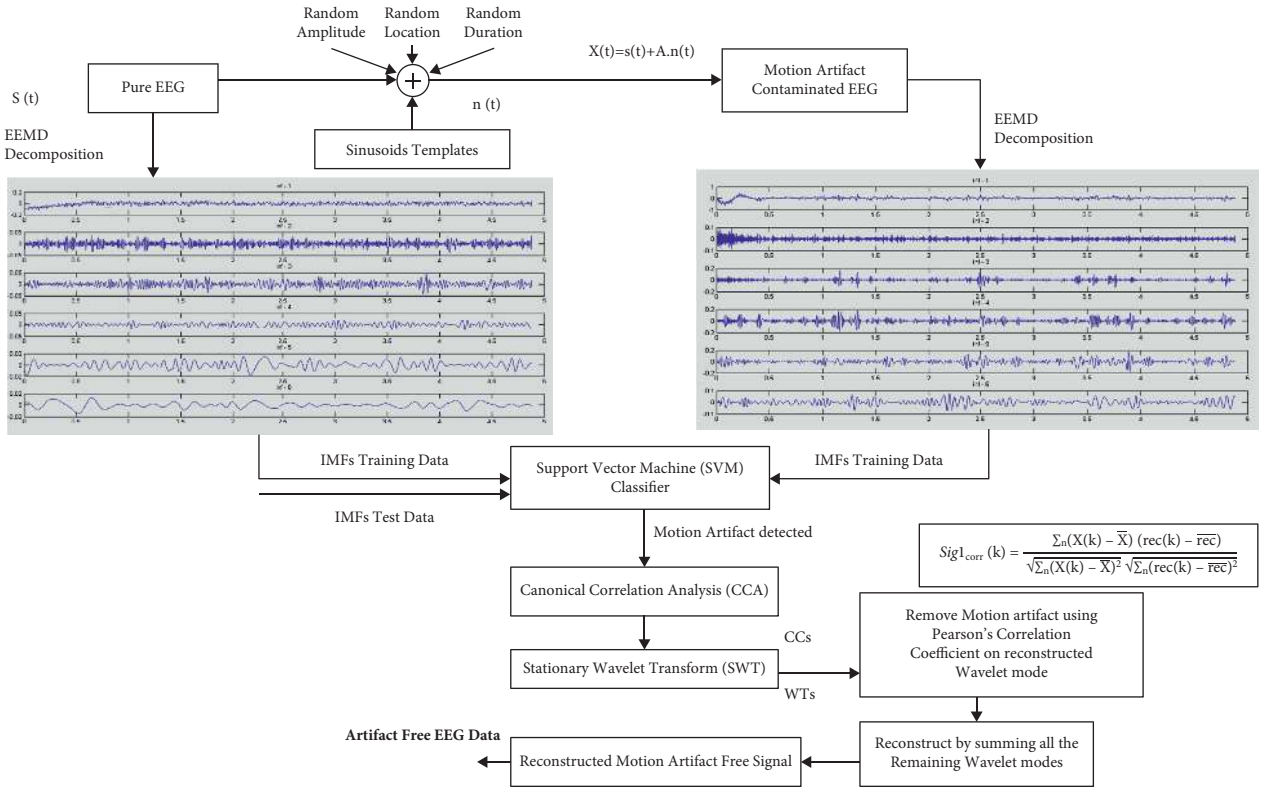

Figure 1: EEG artifacts' removal recommended architecture.

been compared with the existing methodologies whose results are available in state of the art [30]. The data samples are considered from an online open surface interface [22]. The MATLAB code used for EEMD is free to download from [31], and the rest of the functions required are directly used from the Matlab toolbox. Ground-truth EEG signal and synthesized motion artifact simulated EEG signals are shown in Figure 2. This simulated EEG signal is created by adding randomly simulated sinusoids into the original EEG signal at different locations having different amplitudes. Figure 2 shows the change in behaviour due to simulated artifact.

This synthesized EEG signal is decomposed by using EEMD algorithm. The intrinsic mode functions (IMFs) generated through this EEMD algorithm are presented in Figure 3.

These 14 IMFs extracted from EEMD are used to calculate statistical moment-based features such as mean, variance, kurtosis, and skewness. These statistical features are applied to SVM, a machine learning algorithm for artifact detection. The artifact detection by the neural network is applied by authors [19, 20].

As the name suggests, SVM is a classification algorithm based on supervised learning and used for motion artifact detection from nonlinear EEG data. The SVM have different kernels, which enable the nonlinear classification [32]. The attributes are initially extracted from EEMD-generated IMFs for both pure and artifactual EEG data. These structures were applied as a training set for the machine learning classifier. Furthermore, the test set is also created by using EEMD for artifact contaminated EEG data and pure EEG data. These test sets are passed through the classifier for artifact detection based on the training set. The support vector machine (SVM) and radial basis function (RBF) kernel attain satisfactory accuracy for motion artifact detection from contaminated EEG data. The artifact detection accuracy is presented in Table 1, termed as a confusion matrix.

The confusion matrix suggests that only 6 test sets were incorrectly classified as pure EEG data. These datasets are artifact data. Moreover, pure EEG data are misclassified as artifact data for merely 2 instances. The SVM classifier and radial basis function (RBF) kernel attain the accuracy of 98.3% for motion artifact detection from contaminated EEG signals.

Once the motion artifacts are perceived in the input EEG signal, artifact suppression is executed through a cascaded approach. The IMFs extracted from the EEMD approach of artifacted EEG data are applied to BSS-CCA [13]. The separated components after ensemble consequence of EEMD algorithm and CCA algorithm are presented in Figure 4. Each CCs resembles the section of a different source.

The CCs generated after EEMD-CCA cascaded approach is further processed with stationary wavelet transform (SWT) for improved artifact mitigation. This SWT is preferred as this algorithm will suppress the artifact while maintaining the neural information of the EEG signal [33].

In real-time application, the occurrence of artifacts in the recorded EEG data is not known. The recommended algorithm will be quite effective and can be implemented

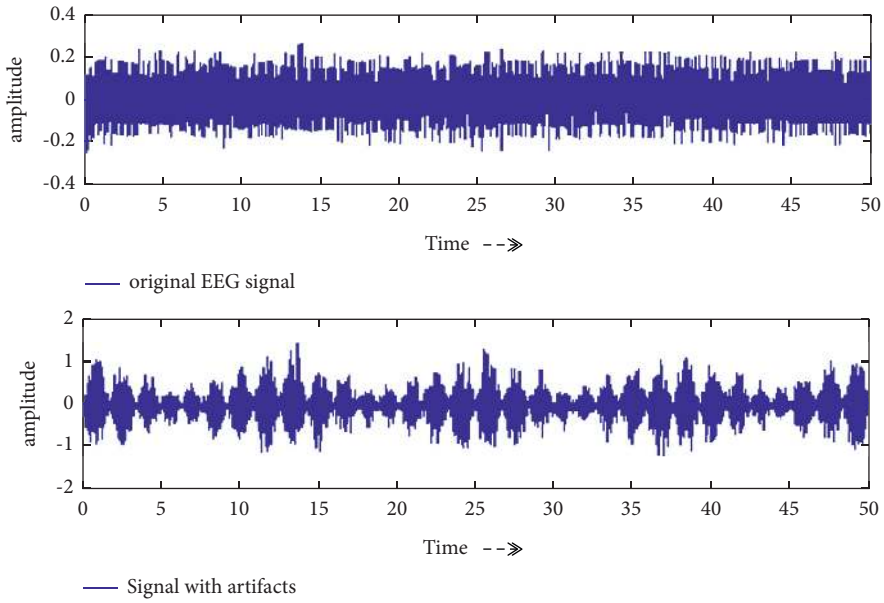

Figure 2: Original and motion artifact-simulated EEG signal.

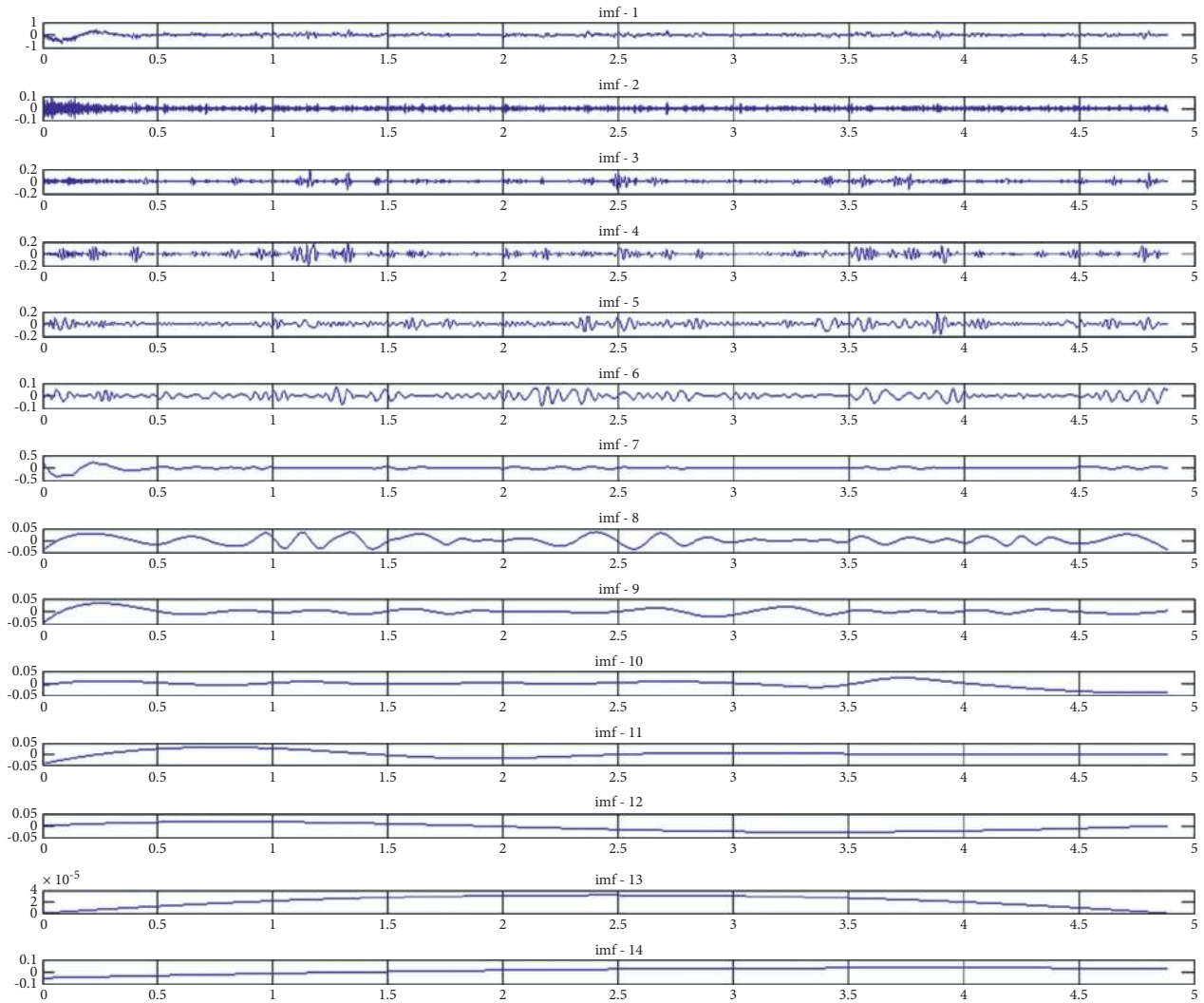

Figure 3: IMFs generated from EEMD algorithm.

Table 1: Artifact detection accuracy confusion matrix.

EEG dataset	Machine scoring		Actual scoring
	Artifact contaminated	Pure	
Artifact contaminated	114	6	120
Pure	2	118	120

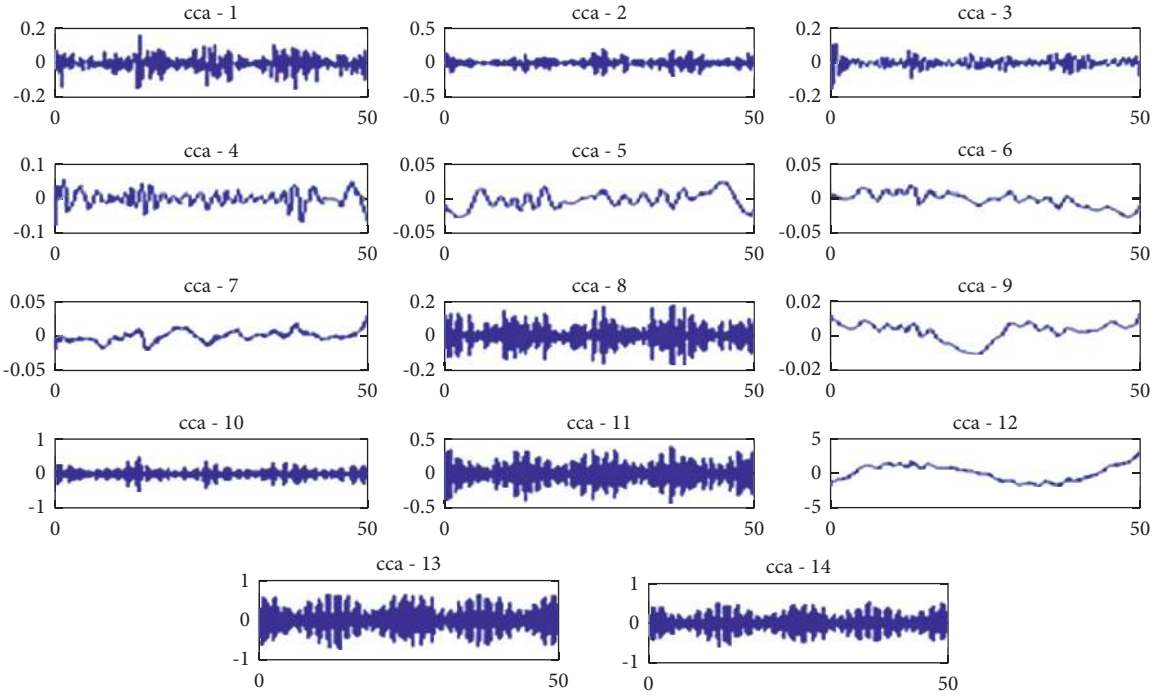

Figure 4: Components generated after EEMD-CCA cascaded approach.

practically. Foremost, first, the motion artifact will be detected through a classification algorithm. Once the artifact is detected, then disturbance created due to motion artifact in EEG signal can be best handled with the efficient and improved artifact removal algorithm (CCA-SWT). As CCA is a simple source separation approach, SWT is preferred as an effective artifact elimination algorithm due to its shift-invariance property [34].

The synthesized EEG data and the reconstructed EEG data (post artifact elimination) comparison is shown in Figure 5.

Figure 5 shows the comparison of the plot for artifactual EEG signal with blue colour and motion artifact suppressed EEG signal by red colour. It can be observed from visual inspection that the EEG signal is dirtied with the great, random motion artifact. The recommended method minimizes these artifacts greatly while preserving all the neural information initially present in the pure EEG signal.

The recommended algorithm is tested on the different EEG datasets to check the validity of the recommended procedure in actual time application. The recommended algorithm effectively detects motion artifactual EEG dataset as shown in Figure 6 in the red box. In addition, EOG artifacts have been minimized significantly. Although, in this work, the SVM classifier is trained for motion artifacts only. The detection ability of the classifier will be improved in future work.

Thus, the motion artifacts have been removed by the recommended method (EEMD-CCA-SWT) as well as preserved by the peak amplitude variations, which carry the required information for the signal. Thus, Figure 6 shows that the recommended method preserves the meaningful information even after artifact removal. A statistical analysis of the recommended method with existing methods is given in Section 4.

4. Performance Assessment Factors

Some important performance evaluation parameters for assessment of the recommended algorithm are as follows.

4.1. Difference in Signal-to-Noise Ratio (SNR). The SNR is calculated by the change of SNR for the signal pre- and postartifact removal [6].

4.2. Lambda. This is a difference in correlation between signals which shows the percentage reduction in artifacts denoted by λ [6].

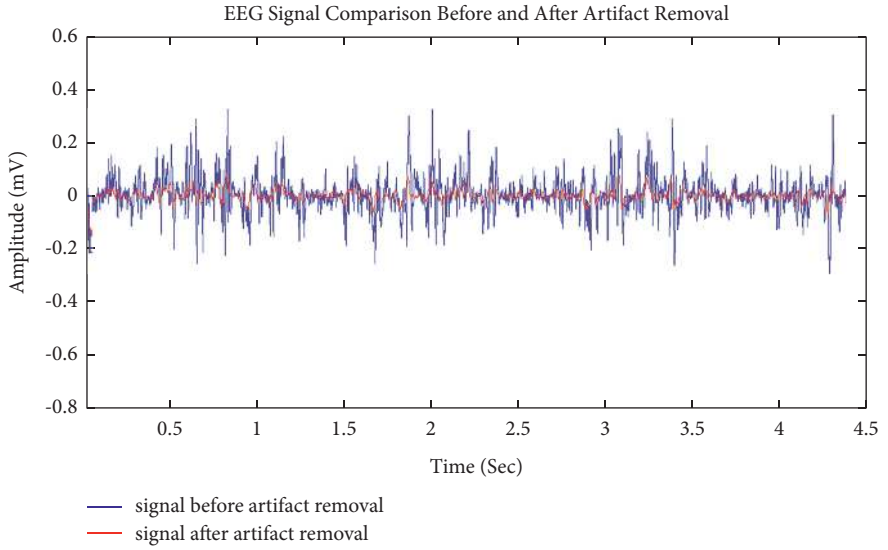

Figure 5: EEG signal comparison before and after artifact removal.

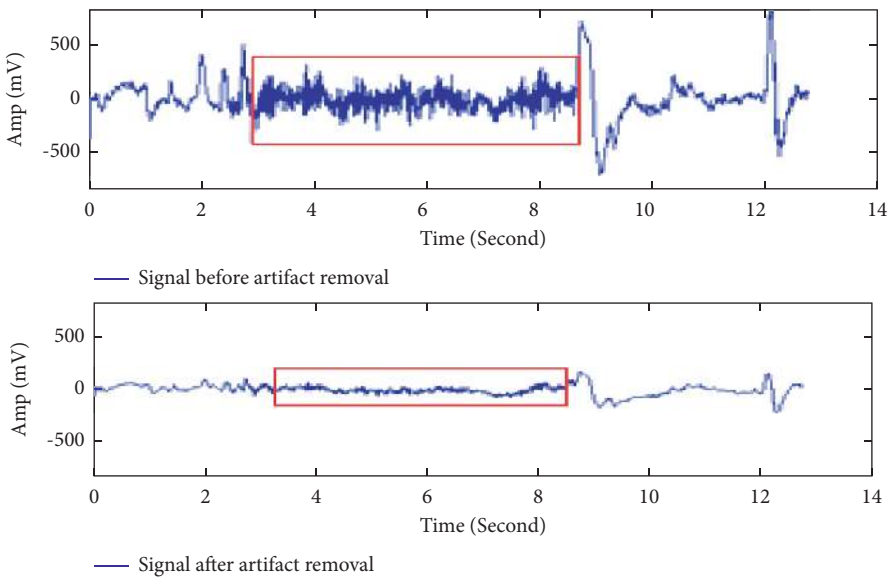

Figure 6: Comparison of synthetic artifact signal and smoothen signal with EEMD-CCA-SWT.

4.3. Power Spectral Density (PSD) Improvement. PSD improvement is calculated by finding the change between PSD of the artifactual and artifact-free data [6].

4.4. Correlation Improvement. The association difference between synthesized and original signal is used as the performance measure.

4.5. Root Mean Square Error (RMSE). The RMSE amongst the ground-truth data, signal along with artifacts (artifactual EEG), and signal postartifact elimination (cleaned EEG) is calculated [6].

4.6. Spectral Distortion (P_{dis}). The spectral distortion P_{dis} is deliberated as

$$P_{\text{dis}} = \frac{\sum \text{PSD}_{\text{recon}}(f)^2}{\sum \text{PSD}_{\text{ref}}(w)^2}, \tag{1}$$

where $\text{PSD}_{\text{ref}}(w)$ denotes PSD of the reference signal and $\text{PSD}_{\text{recon}}(f)$ denotes PSD of the reconstructed signal.

The spectral distortion P_{dis} is given by the PSD ratio of the reconstructed signal to the reference EEG signal [10].

4.7. Coherence Improvement (ΔCoh). ΔCoh measures the phase consistency between noisy and ground-truth signal. The percentage coherence improvement is defined as

$$\zeta = 100 * \frac{(Coh_{\text{afer}} - Coh_{\text{before}})}{Coh_{\text{before}}}. \tag{2}$$

$$\mathscr{E} = 100 * (Coh_{\text{after}} - Coh_{\text{before}})/Coh_{\text{before}}\ \mathscr{E} = d$$

Table 2: Comparison of the recommended method with the existing method for artifact removal.

Methodology	Evaluation parameters	Signal-to-noise ratio (SNR)		
		10	20	25
EEMD-CCA [6]	DSNR	18.611	21.7920	25.4018
Recommended (EEMD-CCA-SWT)		27.2775	32.8229	31.3270
EEMD-CCA [6]	Lambda	63.009	67.5610	71.9953
Recommended (EEMD-CCA-SWT)		75.6307	88.746	87.2213
EEMD-CCA [6]	Correlation improvement	0.0047	0.0060	0.0054
Recommended (EEMD-CCA-SWT)		0.0161	0.0258	0.0140
EEMD-CCA [6]	Spectral distortion (P_{dis})	0.8974	0.9697	0.9487
Recommended (EEMD-CCA-SWT)		0.9640	0.9856	0.9867
EEMD-CCA [6]	RMSE	0.1285	0.1166	0.1072
Recommended (EEMD-CCA-SWT)		0.093	0.1126	0.0974
EEMD-CCA [6]	Coherence improvement (Δ**Coh**) in percentage	84.86	83.10	83.29
Recommended (EEMD-CCA-SWT)		86.93	84.26	85.11

The variable is the coherence between mention and artifactual signals and the coherence between mention and recreated signals [35]. Thus, the higher value of ζ shows the superior artifact removal.

4.8. Information Transfer Rate (ITR). Brain-computer interfaces use the information transfer rate (measured in bits per trial) as an evaluation metric (BCI). One mental-calculation task and two motor-imagery tasks were performed by two subjects. The tasks included left hand, right hand, foot, tongue, and foot. Hidden Markov models are used to classify the electroencephalogram (EEG) patterns. BCI systems with two subsets have their information transfer rates reported. There is a wide variation in the information transfer rates, ranging from 0.46 bits per trial to 0.82 bits per trial.

5. Results and Discussion

The simulation is performed on an available online dataset [22] for statistical evaluation. The synthetic artifacts are added to reference data at random locations and at a random time (stretching from 150 μs to 1 s).

The analysis is based on artifacts' removal and signal distortion. The quantitative evaluations of some important matrices are shown in Table 2. These evaluations are done for synthesized EEG signals generated with different SNRs. Moreover, these results are compared with all existing artifact removal methodology EEMD-CCA [6].

From Table 2, it is manifested that the recommended method performs better than the existing method [6] with improved DSNR, which indicates the improved quality of signal after artifact removal. Moreover, it also indicates that boosted Lambda, correlation, and PSD value show improved artifact removal in assessing the existing approaches. Additionally, the RMSE [36] values have reduced significantly with the recommended artifact removal method. The reduction in the RMSE value indicates effective artifact mitigation from EEG signal [37]. The coherence values have improved after recommended artifact removal presents the efficacy of the approach. Figure 7 shows the plot of RMSE concerning different artifact SNR for EEMD-CCA [6] and EEMD-CCA-SWT artifact removal methods [38].

The recommended artifact removal method has a minimum RMSE value that indicates the significant motion artifact removal. The recommended method performs much better with high artifact SNR. Figure 8 demonstrates the behaviour of spectral distortion for the recommended method and compared with EEMD-CCA. The result shows that restored signal PSD reaches close to the reference signal PSD value with high artifact SNR significantly.

Figures 9 and 10 present the extent of artifact elimination by scheming the DSNR and lambda parameters for different SNRs. It can be concluded that both the parameters have improved [39] with respect to other existing methods. However, results are improved by using latest and accurate optimization algorithm which is discussed in subsequent section.

6. Harris Hawks Optimization (HHO)

Asghar Heidari et al. [40] introduced an innovative population-based, gradient-free optimization method in 2019 [41]. HHO simulates Harris hawks' actions of predation, surprise pounce, and attack. In addition, HHO contains two optimization stages, namely, exploitation and exploration, like other metaheuristic algorithms (see Figure 11) mentioned in the following sections.

6.1. Investigation Stage. Harris hawks have insightful eyes that track and spot predators, but sometimes it is not easy to locate the predators. Then, the Harris hawks will stick, wait, and last hours, waiting patiently. In HHO, above actions are modelled [41] on the stage of discovery as follows:

$$P_i^{t+1} = \begin{cases} P_{\text{rand}}^t - N_1 \left| P_{\text{rand}}^t - 2N_2 P(t) \right|, & x \geq 0.5, \\ \left(P_{\text{rabbit}} - P_m^t\right) - N_3\left(LB + N_4(UB - LB)\right), & x < 0.5, \end{cases} \tag{3}$$

where P_i^{t+1} denotes location of ith individual in $(t+1)$th repetition, P_{rabbit} denotes position of the rabbit (predators), x denotes the arbitrary number in the range [0, 1], N_1, N_2,

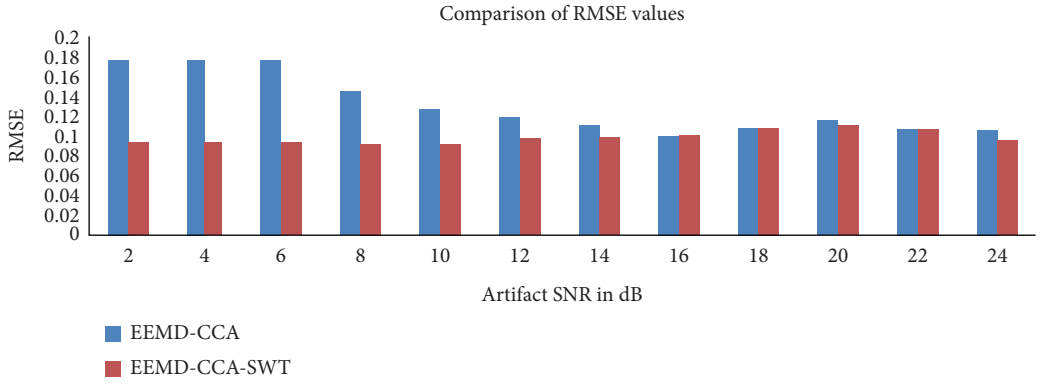

Figure 7: Signal distortion measurement in terms of RMSE for different artifact SNRs.

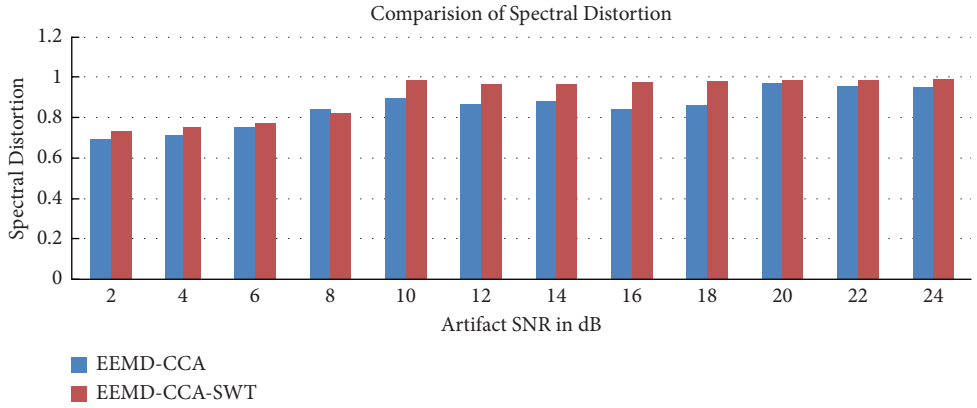

Figure 8: Signal distortion measurement in terms of spectral distortion improvement for different artifact SNRs.

N_3, and N_4 are also random numbers inside [0, 1], LB is the lowest bound of the given optimization problem; UB is the highest bound of the given optimization problem, and P_m^t denotes the middling position of the populace which is calculated as follows:

$$P_m^t = \frac{1}{s}\sum_{i=1}^{M} P_s^t, \tag{4}$$

where M is the extent of the populace and P_s^t is the location of sth specific in ith repetition.

6.2. Evolution from Exploration to Exploitation. The evolution from exploration to use is perilous to metaheuristic approaches [41]. In HHO, rabbit evasion energy is denoted by A and is applied to transform these dual stages. The assessment declines with the rise in the numeral of repetitions, which can be performed arithmetically as

$$A = A_0 * \left(1 - \frac{t}{t_{\max}}\right), \tag{5}$$

where A_0 is an arbitrary number which is defined in the interlude [−1, 1], t represents the current iteration, and $t_{\max}$ characterises the extreme iterations' number.

6.3. Exploitation Stage. Harris hawks also targeted gnaw after they have found their prey [41]. The real process of predation is always very complex, the prey has an escape opportunity, and Harris hawks responded differently according to the prey's behaviour. Four techniques are used in the exploitation stage to better model the actual situation. An arbitrary number (N) is applied to define whether the prey has escaped effectively. Condition $N < 0.5$ designates a good escape, while case $N > 0.5$ shows a loss. The energy absconding from the beast (A) affects the Harris hawks' actions. The soft assault happens if $|A| < 0.5$; if not, then hard assault takes place [41].

When the artifact supressed signal is processed through this Harris hawks optimization process, the irregularity due to external and electronic noise is removed greatly. The mentioned improvement can also be analysed by Table 3.

Table 3 suggests that, after optimization algorithm application, the EEG artifact removal performance is improved. EEG noise is suppressed, while EEG signal quality is preserved.

In this research paper, the recommended artifact removal method performance is measured by both parametric value and plot comparison. Moreover, both approaches present the success of the recommended method. Moreover, recommended methodology with HHO optimization outperforms over other methods.

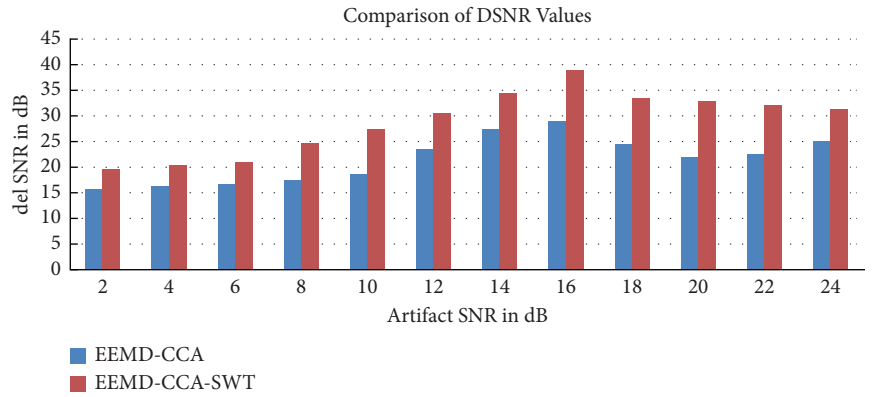

Figure 9: Artifact removal measurement in terms of DSNR for different artifact SNRs.

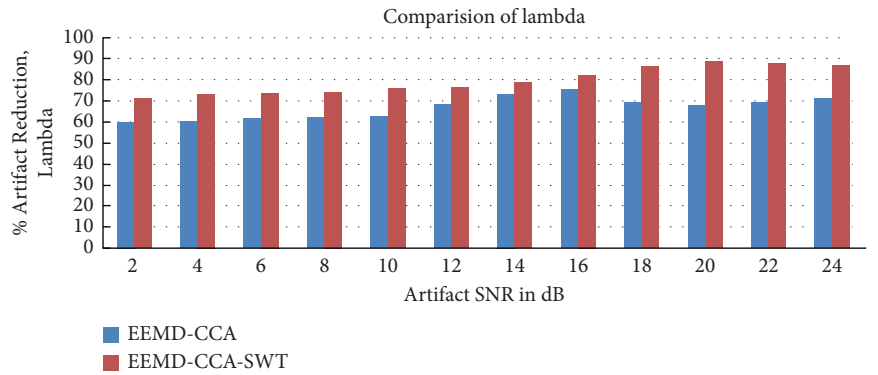

Figure 10: Artifact elimination measurement in terms of Lambda for various artifact SNRs.

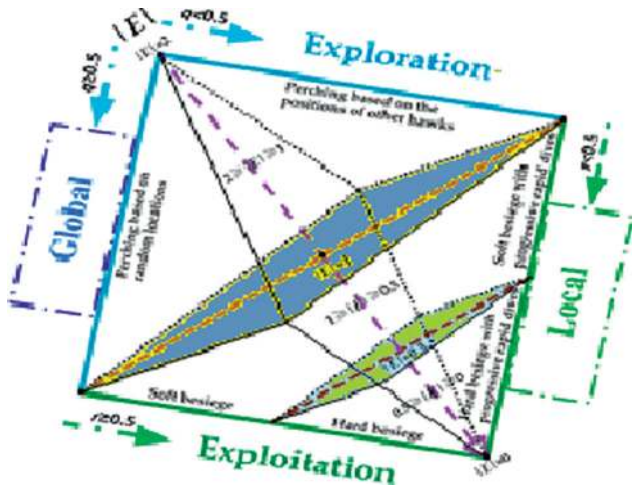

Figure 11: Harris hawks' optimization (HHO) at different stages.

Table 3: Comparison of EEG artifact removal performance before and after optimization.

Methodology	Evaluation parameters	Signal-to-noise ratio (SNR)		
		10	20	25
EEMD-CCA-SWT	DSNR	27.2775	32.8229	31.3270
EEMD-CCA-SWT + HHO		28.2345	34.2475	37.2172

Table 3: Continued.

Methodology	Evaluation parameters	Signal-to-noise ratio (SNR)		
		10	20	25
EEMD-CCA-SWT	Lambda	75.6307	88.746	87.2213
EEMD-CCA-SWT + HHO		78.6307	89.627	89.6127
EEMD-CCA-SWT	Correlation improvement	0.0161	0.0258	0.0140
EEMD-CCA-SWT + HHO		0.0141	0.0261	0.0121
EEMD-CCA-SWT	Spectral distortion (P_{dis})	0.9640	0.9856	0.9867
EEMD-CCA-SWT + HHO		0.9356	0.9756	0.952
EEMD-CCA-SWT	RMSE	0.093	0.1126	0.0974
EEMD-CCA-SWT + HHO		0.091	0.1123	0.0913
EEMD-CCA-SWT	Coherence improvement (Δ**Coh**) in percentage	86.93	84.26	85.11
EEMD-CCA-SWT + HHO		85.82	84.22	83.09

7. Conclusion

In this research work, an effective EEG motion artifact detection and removal approach are recommended for cultivating the precise neurological diseases analysis and diagnosis. Primarily, the signal channel signal is decomposed by using EEMD algorithm. These decomposed EEGs (IMFs) have been applied to SVM classifier for detection of artifacts from input EEG signal. Once artifacts are detected, then efficient artifact removal cascaded approach (CCA-SWT) is applied on IMFs. The correlation coefficients are reconstructed after motion artifact detection and removal. The reconstructed signals are further optimized by HHO algorithm and evaluated qualitatively by visual analysis and quantitatively based on parametric evaluation. The results show improved performance as compared to results on [6] for EEG artifact removal. Moreover, it is also concluded that the neural information are preserved even after artifact suppression.

In the future, we will try to improve the performance of artifact removal method which is adaptive for detection of various neural artifacts, and and improved version of optimization algorithm will be applied to optimize the result.

Data Availability

The data used to support the findings of this study are available from the corresponding author upon request.

Conflicts of Interest

The authors declare that they have no conflicts of interest.

Acknowledgments

The authors are thankful for the support from Taif University Researchers Supporting Project (TURSP-2020/114), Taif University, Taif, Saudi Arabia.

References

[1] K. T. Sweeney, T. E. Ward, and S. F. McLoone, "Artifact removal in physiological signals-practices and possibilities," *IEEE Transactions on Information Technology in Biomedicine*, vol. 16, no. 3, pp. 488–500, 2012.

[2] M. Jansen, T. P. White, K. J. Mullinger et al., "Motion-related artefacts in EEG predict neuronally plausible patterns of activation in fMRI data," *NeuroImage*, vol. 59, no. 1, pp. 261–270, 2012.

[3] F. C. Robertson, T. S. Douglas, and E. M. Meintjes, "Motion artifact removal for functional near infrared spectroscopy: a comparison of methods," *IEEE Transactions on Biomedical Engineering*, vol. 57, no. 6, pp. 1377–1387, 2010.

[4] M. Hassan, S. Boudaoud, J. Terrien, B. Karlsson, and C. Marque, "Combination of canonical correlation analysis and empirical mode decomposition applied to denoising the labor electrohysterogram," *IEEE Transactions on Biomedical Engineering*, vol. 58, no. 9, pp. 2441–2447, 2011.

[5] K. T. Sweeney, H. Ayaz, T. E. Ward, M. Izzetoglu, S. F. McLoone, and B. Onaral, "A methodology for validating artifact removal techniques for physiological signals," *IEEE Transactions on Information Technology in Biomedicine*, vol. 16, no. 5, pp. 918–926, 2012.

[6] K. T. Sweeney, S. F. McLoone, and T. E. Ward, "The use of ensemble empirical mode decomposition with canonical correlation analysis as a novel artifact removal technique," *IEEE Transactions on Biomedical Engineering*, 2013.

[7] M. C. Anastasiadou and G. D. Mitsis, "Automatic detection and removal of muscle artifacts from scalp EEG recordings in patients with epilepsy," *Engineering in Medicine and Biology Society*, pp. 1946–1950, 2015.

[8] N. E. Huang, Z. Shen, S. R. Long et al., "The empirical mode decomposition and the Hilbert spectrum for nonlinear and non-stationary time series analysis," *Proceedings of the Royal Society of London. Series A: Mathematical, Physical and Engineering Sciences*, vol. 454, no. 1971, pp. 903–995, 1998.

[9] Z. Wu and N. E. Huang, "Ensemble empirical mode decomposition: a noise-assisted data analysis method," *Advances in Adaptive Data Analysis*, vol. 1, no. 1, pp. 1–41, 2009.

[10] M. K. Islam, A. Rastegarnia, A. T. Nguyen, and Z. Yang, "Artifact characterization and removal for in vivo neural recording," *Journal of Neuroscience Methods*, vol. 226, pp. 110–123, 2014.

[11] A. Oja and O. Erkki, "A fast fixed-point algorithm for independent component analysis," *Neural Computation*, vol. 9, no. 7, pp. 1483–1492, 1997.

[12] S. Arora, R. Ge, A. Moitra, and S. Sachdeva, "Provable ICA with unknown Gaussian noise, with implications for Gaussian mixtures and autoencoders," *Advances in Neural Information Processing Systems*, pp. 2375–2383, 2012.

[13] H. Hotelling, "Relations between two sets of variates," *Biometrika*, vol. 28, no. 3-4, pp. 321–377, 1936.

[14] O. Friman, M. Borga, P. Lundberg, and H. Knutsson, "Exploratory fMRI analysis by autocorrelation maximization," *NeuroImage*, vol. 16, no. 2, pp. 454–464, 2002.

[15] D. Safieddine, A. Kachenoura, L. Albera et al., "Removal of muscle artifact from EEG data: comparison between stochastic (ICA and CCA) and deterministic (EMD and wavelet-based) approaches," *EURASIP Journal on Applied Signal Processing*, vol. 127, no. 1, pp. 1–15, 2012.

[16] P. S. Kumar, R. Arumuganathan, K. Sivakumar, and C. Vimal, "Removal of ocular artifacts in the EEG through wavelet transform without using an EOG reference channel," *Int. J. Open Problems Compt. Math*, vol. 1, no. 3, pp. 188–200, 2008.

[17] P. Quan Pan, Z. Lei Zhang, D. Hongai Zhang, and Z. Hongai, "Two denoising methods by wavelet transform," *IEEE Transactions on Signal Processing*, vol. 47, no. 12, pp. 3401–3406, 1999.

[18] N. Al-Qazzaz, S. Hamid Bin Mohd Ali, S. Ahmad, M. Islam, and J. Escudero, "Selection of mother wavelet functions for multi-channel EEG signal analysis during a working memory task," *Sensors*, vol. 15, no. 11, pp. 29015–29035, 2015.

[19] H.-A. T. Nguyen, J. Musson, F. Li et al., "EOG Artifact removal using a wavelet neural network," *Neurocomputing*, vol. 97, pp. 374–389, 2012.

[20] C. Burger and D. J. van den Heever, "Removal of EOG artefacts by combining wavelet neural network and independent component analysis," *Biomedical Signal Processing and Control*, vol. 15, pp. 67–79, 2015.

[21] R. Vandana and S. Shailja, "A methodical healthcare model to eliminate motion artifacts from big EEG data," *Journal of Organizational and End User Computing*, vol. 29, no. 4, pp. 84–102, 2016.

[22] "PhysioNet-motion artifact contaminated EEG and EEG data (motion artifact)," http://physionet.org/cgi-bin/atm/ATM.

[23] V. Roy, S. Shukla, P. K. Shukla, and P. Rawat, ""Gaussian elimination-based novel canonical correlation analysis method for EEG motion artifact removal", advancements of image processing and vision in healthcare," *Hindawi Journal of Healthcare Engineering*, vol. 2017, p. 11, Article ID 9674712, 2017.

[24] S. Pandit, P. K. Shukla, A. Tiwari, P. K. Shukla, M. Maheshwari, and R. Dubey, "Review of video compression techniques based on fractal transform function and swarm intelligence," *International Journal of Modern Physics B*, vol. 34, no. 8, p. 2050061, 2020.

[25] Y. Pathak, P. K. Shukla, and K. V. Arya, "Deep bidirectional classification model for COVID-19 disease infected patients," *IEEE/ACM Transactions on Computational Biology and Bioinformatics*, vol. 18, no. 4, pp. 1234–1241, 2021.

[26] A. Kumar Saxena, S. Sinha, S. Sinha, and P. Shukla, "Design and development of image security technique by using cryptography and steganography: a combine approach," *International Journal of Image, Graphics and Signal Processing*, vol. 10, no. 4, pp. 13–21, 2018.

[27] H. S. Pannu, D. Singh, and A. K. Malhi, "Multi-objective particle swarm optimization-based adaptive neuro-fuzzy inference system for benzene monitoring," *Neural Computing & Applications*, vol. 31, no. 7, pp. 2195–2205, 2019.

[28] Bo Li, L. Zhang, Q. Zhang, and S. Yang, "An EEMD-based denoising method for seismic signal of high arch dam combining wavelet with singular spectrum analysis," *Shock and Vibration*, vol. 2019, Article ID 4937595, 9 pages, 2019.

[29] W. C. Chang and C. Im, "Detection of eye blink artifacts from single prefrontal channel electroencephalogram," *Computer Methods and Programs in Biomedicine*, vol. 124, pp. 19–30, 2015.

[30] D. Singh, J. Singh, and A. Chhabra, "High availability of clouds: failover strategies for cloud computing using integrated checkpointing algorithms," in *Proceedings of the 2012 International Conference on Communication Systems and Network Technologies*, pp. 698–703, Gujrat, India, May 2012.

[31] "EEMD Matlab code," http://perso.ens-lyon.fr/patrick.flandrin/emd.html.

[32] A. R. Hassan and M. I. Hassan Bhuiyan, "Automatic sleep scoring using statistical features in the EMD domain and ensemble methods," *Biocybernetics and Biomedical Engineering*, vol. 36, no. 1, pp. 248–255, 2016.

[33] S. Khatun, R. Mahajan, and B. I. Morshed, "Comparative analysis of wavelet based approaches for reliable removal of ocular artifacts from single channel EEG," *Electro/Information Technology (EIT)*, pp. 335–340, 2015.

[34] H. Ghandeharion and A. Erfanian, "A fully automatic ocular artifact suppression from EEG data using higher order statistics: improved performance by wavelet analysis," *Medical Engineering & Physics*, vol. 32, no. 7, pp. 720–729, 2010.

[35] M. K. Islam, A. Rastegarnia, and Z. Yang, "A Wavelet-Based Artifact reduction from scalp EEG for epileptic seizer detection," *IEEE Journal of Biomedical and Health Informatics*, 2015.

[36] D. Singh and V. Kumar, "A comprehensive review of computational dehazing techniques," *Archives of Computational Methods in Engineering*, vol. 26, no. 5, pp. 1395–1413, 2019.

[37] M. Gupta, N. Kumar, B. K. Singh, and N. Gupta, ""NSGA-III-Based deep-learning model for biomedical search engines,", special issue on deep transfer learning models for complex multimedia applications," *Hindawi Mathematical Problems in Engineering*, vol. 2021, Article ID 9935862, 8 pages, 2021.

[38] A. Dixit, A. Tiwari, and R. K. Gupta, "A model for trend analysis in the online shopping scenario using multilevel hesitation pattern mining," *Hindawi Mathematical Problems in Engineering*, vol. 2021, Article ID 2828262, 11 pages, 2021.

[39] S. Shukla, V. Roy, and A. Prakash, "Wavelet based empirical approach to mitigate the effect of motion artifacts from EEG signal," in *Proceedings of the 2020 IEEE 9th International Conference on Communication Systems and Network Technologies (CSNT)*, pp. 323–326, Gwalior, India, April 2020.

[40] A. Asghar Heidari, S. Mirjalili, H. Faris, I. Aljarah, M. Mafarja, and H. Chen, "Harris hawks optimization: Algorithm and applications," *Future Generation Computer Systems*, vol. 97, 2019.

[41] A. A. Heidari, S. Mirjalili, H. Faris, I. Aljarah, M. Mafarja, and H. Chen, "Harris hawks optimization: algorithm and applications," *Future Generation Computer Systems*, vol. 97, pp. 849–872, 2019.